

EFFECT OF OXIDATION AND HYDROXYPROPYLATION ON STRUCTURE AND PROPERTIES OF HIGH-AMYLOSE CORN STARCH, AND PREPARATION OF HYDROXYPROPYL OXIDIZED HIGH-AMYLOSE CORN STARCH

TANG HONGBO, PAN KUN, LI YANPING and DONG SIQING

Science School, Shenyang University of Technology, Shenyang 110870, China

✉ *Corresponding author: Tang Hongbo, tanghb6666@sina.com*

Received February 8, 2017

The aim of this study was to investigate the effect of oxidation and hydroxypropylation on the structure and properties of high-amylose corn starch (HACS) by means of Fourier transform infrared spectroscopy (FTIR), differential scanning calorimetry (DSC), thermogravimetric analysis (TGA), X-ray diffraction (XRD), scanning electron microscopy (SEM) and energy dispersive X-ray analysis (EDAX). The crystalline structure of HACS belonged to the A type, while the amorphous region of HACS granules was mainly located on the side face. The manner of the oxidation was different from that of the hydroxypropylation for HACS. The oxidation mainly occurred in the crystalline region, whereas the hydroxypropylation mainly occurred in the amorphous region. The hydroxypropylation occurred unevenly on granules. The oxidation could enhance the blue value of HACS from 0.537 to 0.725. However, the blue value of HACS was not basically influenced by the hydroxypropylation. The oxidation and hydroxypropylation could improve the acid and alkali resistance, cold and hot viscosity stability of HACS. The oxidation and hydroxypropylation changed the thermal stability and melting process of HACS, that is, the difference in the enthalpy change between HACS and hydroxypropylated oxidized high-amylose corn starch (HOHACS) reached 75.1 J/g.

Keywords: starch, oxidation, hydroxypropylation, structure, property, optimization

INTRODUCTION

Starch is a natural polymer made of amylose, a linear polymer of α -(1-4) glucose units, and amylopectin, a branched polymer of α -(1-4) linear glucose units, with periodic branches of α -(1-6) linkages.¹ It is extracted from several sources as semi-crystalline granules with different shapes and diameters. Unlike normal starches, the starches from the amylose extended mutants of barley or maize unusually have high amylose

content from 40 to 70%. These starches display unique physical characteristics, such as resistance to swelling, resistance to digestion, rapid gelling *etc.*² High-amylose corn starch (HACS) is known to produce strong, flexible films, probably due to amylose crystallization.³ However, it still has some limitations in the native form.

Chemical modification will provide an efficient route not only for removing some

drawbacks of HACS, but also for improving its expansibility and solubility.

Oxidation, as a chemical way of starch modification, is commonly used to obtain modified starches with the low viscosity at high solid concentrations. In the case of oxidized starches, they present low hot paste viscosity due to the partial degradation of the macromolecules, as well as low tendency towards syneresis due to the presence of the carbonyl and carboxyl groups.⁴ Currently, hypochlorite oxidation is the most common method for the production of oxidized starches on an industrial scale. The oxidation is usually performed in alkaline environment in order to favor the yield of carboxyl groups. In commercial conversions, sodium or calcium hypochlorite is usually used as an oxidizing agent.⁵

In recent years, oxidized starches have attracted much interest and have become widely used in many industries.⁶ Due to their neutral taste and low viscosity, oxidized starches are applied as a food ingredient in food products, such as salad cream, as dough conditioner for bread and as sealing agent in confectionaries *etc.*⁷ In the paper industry, it can be used as sizing agent and coating agent, which will enhance the tension of the paper, improve the strength of the paper surface and its printing function. It is also used as an emulsifier, as a substitute for arabic gum and a binding agent in the batter application.⁸

Hydroxypropylation is an etherification process that is commonly used to modify the starch and results in granules swelling due to the high water penetration inside the starch granules. The hydroxypropyl groups break the hydrogen bond in starch, leading to greater flexibility of the granules and decreasing paste stability.⁹ Thereby, the hydroxypropylation of starches is used to improve the stability of starch-based products during low temperature storage.

However, little research has been focused on

preparing hydroxypropylated oxidized high-amylose corn starch (HOHACS). On the basis of the above background, in this study, HOHACS was synthesized by the aqueous phase method to keep the basic structure of native starch particles.

The effect of the reaction conditions, including the amount of oxidant, reaction temperature, pH and reaction time, on the carboxyl content was thoroughly discussed. The optimum conditions for preparing HOHACS were established based on response surface methodology.

EXPERIMENTAL

Materials

High-amylose corn starch (Amylose content 70%) was purchased from Shandong Huanong Special Corn Development Co. Ltd. (China). Sodium hypochlorite (active chlorine content 10%) was obtained from Shenyang Chemical Industry Co. Ltd. (China). Propylene oxide was received from Sinopharm Chemical Reagent Co. Ltd. (China). Sodium hydroxide was bought from Shenyang Xinhua Reagent Factory (China). Hydrochloric acid was purchased from Shenyang Technological Development Zone Reagent Factory (China). Sodium sulfite was obtained from Shenyang Reagent Factory (China). Anhydrous sodium sulfate purchased from Shenyang Dongxing Reagent Factory (China). All the above reagents were of analytical grade, except for the sodium hypochlorite.

Methods

Preparation of oxidized high-amylose corn starch (OHACS)

A starch slurry with the mass concentration of 40% was produced by adding 30 g of precisely weighed HACS (dry basis) and 45 g of distilled water, and then put into a 250 mL three-neck flask, equipped with a mechanical stirrer and a heating device. The resultant slurry was heated to the required temperature, and the pH was adjusted to 9 with 1 mol/L sodium

hydroxide solution. A quantity of the sodium hypochlorite, whose effective chlorine content was 10%, was then slowly dropped into the slurry during 30 min, while maintaining the pH of the slurry at 9 with 1 mol/L sodium hydroxide solution. After that, 1 g of sodium sulfite was added to stop the reaction, and then the pH of the slurry was adjusted to 6.0-7.0 by adding 0.5 mol/L hydrochloric acid solution. The vacuum filtration of the slurry was completed by a SHZ-C vacuum pump with a circulated water system (Henan Province Gongyi City, YingYuHua Instrument Factory, China). The filtered cake was then washed more than four times with distilled water. The resultant cake was dried at 100 °C. The dry cake was ground and screened. Finally, the OHACS was obtained.¹⁰

Preparation of hydroxypropylated oxidized high-amylose corn starch (HOHACS)

A slurry with the mass concentration of 40% was produced by adding 30 g of OHACS (dry basis) weighed precisely and 45 g of distilled water, and then put into a 250 mL three-necked flask, stirred, and heated to the required temperature in a water bath. A quantity of anhydrous sodium sulfate was added into the slurry. After constant temperature was kept for 10 minutes, a quantity of sodium hydroxide was slowly added into the slurry. Then, a quantity of epoxy propane was quickly added. The hydroxypropylation reaction was carried out for 18 h in a three-necked flask with a reflux device. After the reaction ended, the pH of the slurry was neutralized to 6.0-7.0 by the hydrochloric acid solution with a mass concentration

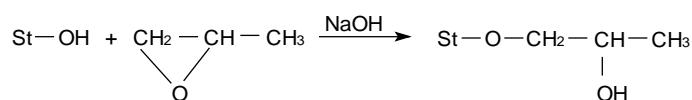
of 10%. The slurry was filtered by a SHZ-C vacuum pump with a circulated water system (Henan Province Gongyi City, YingYuHua Instrument Factory, China). The obtained cake was washed more than four times by distilled water, and then dried, pulverized and sieved, so that HOHACS was obtained.¹¹ Under alkaline conditions, the etherification formula of OHACS reacting with the epoxy propane is in Scheme 1.

Carboxyl content

About 5 g of sample was mixed with 25 mL of 0.1 mol/L HCl, and the slurry was stirred continuously for 30 min with a magnetic stirrer. After that, the slurry was filtrated. The cake was washed by distilled water until the chlorine ions were removed completely. The slurry was prepared by adding the above cake and 300 g of distilled water into an Erlenmeyer flask, and heating it to boiling temperature with continuous stirring until gelatinization was achieved. Then, it was titrated with a standardized 0.01 mol/L NaOH solution to the pH of 8.3. A blank was prepared using native starch. All the samples were measured three times. The carboxyl content was calculated as follows:¹²

$$CC = \frac{(V_1 - V_2) \times M \times 0.045}{m} \times 100\% \quad (1)$$

where CC is the carboxyl content (%), m is the mass of the dry samples, V₁ is the volume of 0.01 mol/L NaOH used to titrate the samples (mL), V₂ is the volume of 0.01 mol/L NaOH used to titrate the blank (mL), M is the concentration of NaOH.



Scheme 1: Etherification of starch

Molar substitution (MS)

The principle of the substitution degree determination of the samples was based on propylene glycol. An amount of 0.05 to 0.1 g of the samples weighed

accurately was put into a volumetric flask. Then, 25 mL of 0.5 mol/L sulfuric acid was added into the flask. The mixture was heated in a boiling water bath until the samples were dispersed in the transparent solution.

The solution was cooled to the room temperature, diluted to 100 mL with distilled water. 1 mL of the solution was pipetted into a 25 mL graduated test tube, and the tube was immersed in water. 8 mL of the concentrated sulphuric acid was added to dropwise the tube and shaken well. The tube was heated in the boiling water bath for 3 min and then immediately cooled to 5 °C in an ice water bath. Then, 0.5 mL of ninhydrin solution was added to it, it was shaken well and maintained at a constant temperature of 25 °C for 100 min. The solution was then made up to 25 mL with concentrated sulphuric acid, thoroughly mixed and transferred to a 1 cm cell of the spectrophotometer for 5 min. The absorbance was measured by a WFJ 7200 type spectrophotometer (Unico Instrument Co., Ltd., China) at the wavelength of 595 nm. The starch blank was used as a reference. A calibration curve was prepared with an aliquot (1 mL) of the standard aqueous solutions containing 10, 20, 30, 40 and 50 µg of propylene glycol per mL. The equation of the standard curve was expressed as follows:

$$\text{Absorbance} = -0.0194 + 0.00812 \times \text{propylene glycol concentration } (\mu\text{g/mL}) \quad (2)$$

The propylene glycol content in the samples was calculated from the standard curve, converted to the equivalent hydroxypropyl groups from each molar solution using the following equation. The value of converting the propylene glycol into the hydroxypropyl is 0.7763.¹³

$$H = F \left(\frac{M_{\text{sample}}}{W_{\text{sample}}} - \frac{M_{\text{blank}}}{W_{\text{blank}}} \right) \times 0.7763 \times 100 \quad (3)$$

$$MS = \frac{2.79H}{100 - H} \quad (4)$$

where MS is the molar substitution degree, H is the hydroxypropyl content (%), F is the dilution multiple of samples, and F is equal to 100, M_{sample} is the propylene glycol content of the samples obtained from the standard curve (g), W_{sample} is the quality of the samples (g), M_{blank} is the propylene glycol content of the blank samples obtained from the standard curve (g), W_{blank} is the mass of the blank samples (g).

Blue value

An amount of 100 mL of starch slurry with 0.5 mg/mL was gelatinized by heating in the water bath, then cooled to room temperature. 2 mL of the paste was sucked and placed into a 100 mL volumetric flask. An amount of 0.14-0.2 g of potassium bitartrate and 1 mL of I₂/KI solution (iodine concentration of 2 mg/mL, potassium iodide concentration of 20 mg/mL) were added into the paste, and then diluted by distilled water to 100 mL. The paste was homogenized. The absorbance of the paste was measured at 680 nm by a VI-1501 spectrophotometer (Tianjin Gangdong Sci. & Tech. Development Co., Ltd., China) after the paste was allowed to rest for 60 minutes. The blue value was determined from the following formula:^{14,15}

$$\text{Blue value} = \frac{4 \times \text{absorbance value}}{10 \times \text{sample concentration}} \quad (5)$$

where the unit of the sample concentration is mg/L.

Swelling power

An amount of 0.1 g of precisely weighed dry samples was added into a pre-weighed 10 mL centrifugal tube, and then distilled water was added to give a total volume of water equivalent to 9.9 g. The centrifugal tube was placed in the water bath with the temperature controlled at 85 °C and shaken continuously for 15 min. The volume of the slurry would be kept at this level during the gelatinization. The paste was then cooled to 25 °C. After capping, the centrifugal tube was centrifuged in a TDL80-2B desk centrifuge (Shanghai Anting Scientific Instrument Factory, China) at 3500 r/min for 5 min. The dried residue was then cooled in a desiccator and weighed for the soluble samples. To measure the swelling power, the residual supernatant was carefully removed and discarded. The bottle with the sediment paste was then weighed to give the weight of the swollen sample granules. The results were expressed by the calculation as:^{16,17}

$$\text{Swelling power}(\%) = \frac{\text{weight of sediment paste} \times 100}{\text{weight of sample on dry basis} (100 - \% \text{ solubility})}$$

$$\text{Solubility}(\%) = \frac{\text{weight of dried residue of supernatant} \times 100}{\text{weight of sample on dry basis}}$$

Freeze-thaw stability

The slurry of samples was produced by mixing 0.5 g of dry samples with 99.5 g of distilled water, and then heated up to 95 °C in a 100 mL beaker and kept at this temperature for 10 min before cooling to the ambient temperature. 10 g of the sample paste, which was precisely weighed, was added to each of the preweighed 10 mL centrifuge tubes, and then the sample paste was frozen at -18 °C for 24 h in a BCD-177A refrigerator (Hefei Meiling Co., Ltd., China). The tubes were removed from the freezer and thawed at 25 °C in a water bath for 2 h. Two tubes from each thawing cycle of these samples were centrifuged at 3500 rpm for 15 min. The clear liquid was decanted and the residue was weighed. The separated water percentage was then calculated as the ratio of the mass of the liquid decanted to the total mass of the paste before the centrifugation and multiplied by 100. The lower the separated water percentage, the higher was the freeze-thaw stability.¹⁸⁻²⁰

Acid resistance and alkali resistance

The sample paste with a mass concentration of 1% (w/w) by dry starch or its derivative was produced using distilled water. The sample paste was heated in a boiling bath under constant agitation until it became a complete paste. Then, the paste was cooled in cold water to the required temperature. The pH of the paste was adjusted to 10 or 3, respectively, and the paste was stirred by a glass bar for 5 min. The paste viscosity was then measured by a NDJ-1 rotary viscometer (Shanghai Tianping Instrument Factory, China) at constant temperature (25 °C). The viscosity of the sample changed slightly, which meant strong acid resistance and alkali resistance.^{21,22}

Stability of hot and cold viscosity

The viscosity was measured by a NDJ-1A rotational viscometer (Shanghai Balance Instrument Factory, China). The cold viscosity and hot viscosity were defined as the viscosity of a sample measured at

50 °C and 95 °C, respectively. The stability of the viscosity was determined by the following formula:

$$\text{Stability of viscosity (\%)} = 100 - \text{FRV} \quad (8)$$

The fluctuation ratio of the viscosity was expressed as:

$$\text{FRV (\%)} = \frac{\max|\eta - \eta'|}{\eta''} \times 100 \quad (9)$$

where FRV is the fluctuation ratio of the viscosity (%), η'' is the viscosity measured by keeping the temperature constant for 1 hour at 95 °C or 50 °C, $\max|\eta - \eta'|$ is the maximum viscosity difference measured by keeping the temperature constant for 60 min, 90 min, 120 min, 150 min and 180 min at 50 °C or 95 °C, respectively.²²

Fourier transform infrared spectroscopy (FTIR)

FTIR spectra of the samples were recorded by an IR Prestige-21 infrared spectrometer (Shimadzu Corporation, Japan) in the wavenumber range from 4000 to 400 cm^{-1} . The samples were kept in a vacuum oven at 60 °C for 72 h to remove the absorbed water before the measurement. The resolution was 4 cm^{-1} . The scanning number was 32.²³

TGA and DSC

The thermal analysis of the samples was carried out with a TGA Q50V20.10 Build 36 thermogravimetric analyzer and a DSC Q20 V24.4 Build 116 differential scanning calorimeter (TA Instruments, USA) in a nitrogen atmosphere.

Analysis conditions of TGA: mass of samples – 15.0-16.0 mg, heating rate – 10 °C/min, temperature range – 10-800 °C.²⁴

Analysis conditions of DSC: mass of samples – 4.0-5.0 mg, heating rate – 10 °C/min, temperature range – 10-250 °C.^{25,26}

X-ray diffraction

XRD patterns were obtained using an X'Pert Pro MPD X-ray diffractometer (PANalytical Co., Ltd., Holland). The conditions for recording were as follows: voltage – 40 kV, current – 30 mA, scanning rate –

8°/min and scanning angle (2 θ) – 5-45°. The statistical analysis of the area was performed by MDI Jade 6.5 software. The crystallization degree was calculated as follows:²⁷

$$CD = \frac{A_c}{A_c + A_a} \times 100 \quad (10)$$

where *CD* is the relative crystallization degree (%), *A_c* is the crystalline region area (mm²), and *A_a* is the amorphous area (mm²).

Morphology of particles

The morphology of the particles was observed and analyzed by a Hitachi S-3400N scanning electron microscope equipped with an attached X-ray energy dispersive spectrometer (Hitachi, Ltd., Japan). After drying, the samples in required size and shape were fixed on a carbon coated tape placed on an aluminum stub, then placed in a sputter coater unit and sputtered for 90 s with gold. After coating was over, the samples were observed by a Hitachi S-3400N scanning electron microscope. The scanning was performed in the secondary electron mode at a voltage of 20 or 25 KV.²⁸

Statistical analysis

The statistical significance was assessed with one-way analysis of variance using Design-Expert software 8.05b for Windows program. The most significant difference was considered at $P \leq 0.001$ and a significant difference – at $P \leq 0.05$.

RESULTS AND DISCUSSION

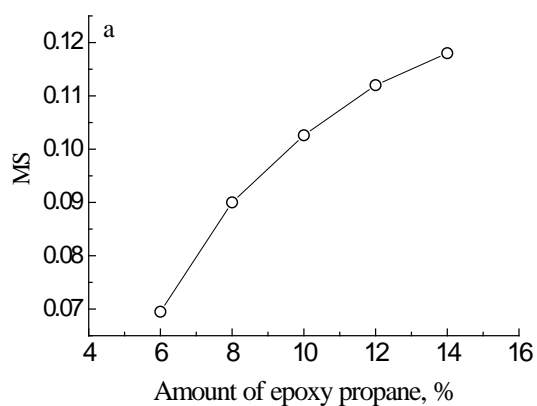
Effect of amount of epoxy propane, sodium hydroxide and sodium sulfate, reaction time and reaction temperature on MS of HOHACS

The effect of the amount of epoxy propane, sodium hydroxide and sodium sulfate, of reaction time and reaction temperature on MS of HOHACS is shown in Figure 1. The amounts of epoxy propane, sodium hydroxide and sodium sulfate were defined as the percentage of the mass ratio of epoxy propane, sodium hydroxide and sodium sulfate to the dry OHACS, respectively.

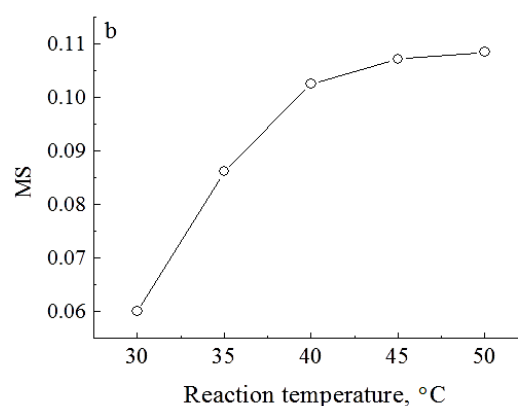
From Figure 1a, the MS of HOHACS increased with increasing the amount of epoxy propane. The MS of HOHACS increased rapidly when the amount of epoxy propane was greater than 8%, while the increasing rate of the MS slowed down when the amount of epoxy propane > 8%. So, the amount of epoxy propane was selected to be 10% by considering the actual use of HOHACS.

As may be noted in Figure 1b, the reaction temperature was varied from 30 to 50 °C to examine the reaction temperature effects. The MS of HOHACS increased with increasing the reaction temperature when the reaction temperature was less than 40 °C. The MS of HOHACS could not increase basically when the reaction temperature was greater than 40 °C. It suggested that the increase in the reaction temperature was favorable for the hydroxypropylation up to 40 °C. On the one hand, high reaction temperature resulted in quickening epoxy propane molecules, which promoted more epoxy propane to react with the starch. On the one hand, the side reaction of epoxy propane and the swelling of starch particles increased with increasing the reaction temperature. As a result, the increase in the movement velocity of epoxy propane molecules could counteract its side reaction and the swelling of starch particles. Thus, the most suitable reaction temperature was considered to be 40 °C.

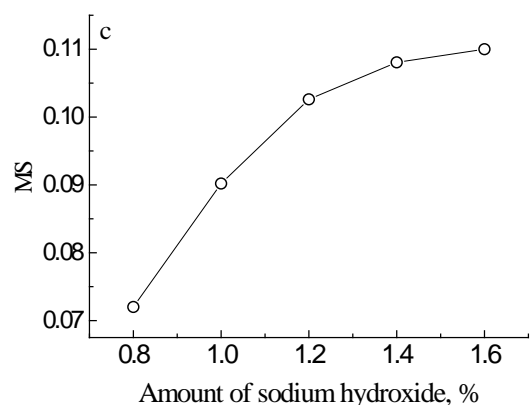
As may be seen in Figure 1c, the reaction time was varied from 10 to 26 h to examine the reaction time effects. The MS of HOHACS increased with increasing the reaction time, when the reaction time was less than 18 h. The MS of HOHACS could not further increase basically when the reaction time was greater than 18 h. As a result, the most suitable reaction time was considered to be 18 h.



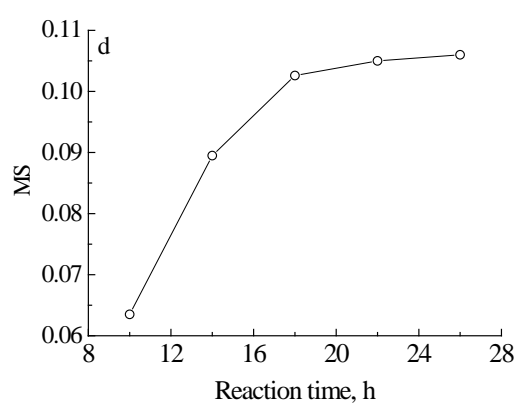
Reaction conditions: reaction time – 18 h, reaction temperature – 40 °C, amount of sodium hydroxide – 1.2%, amount of sodium sulfate – 12%



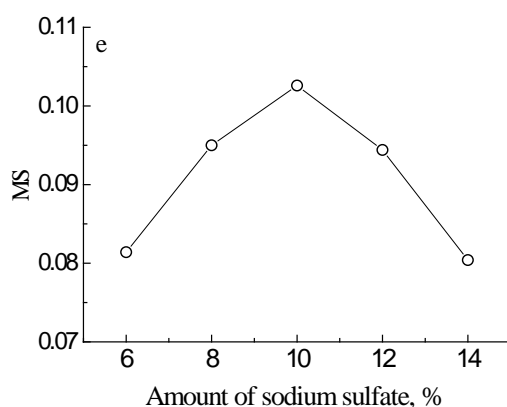
Reaction conditions: reaction time – 18 h, amount of sodium sulfate – 12%, amount of sodium hydroxide – 1.2%, amount of epoxy propane – 10%



Reaction conditions: amount of epoxy propane – 10%, reaction temperature – 40 °C, reaction time – 18 h, amount of sodium sulfate – 12%



Reaction conditions: amount of epoxy propane – 10%, reaction temperature – 40 °C, amount of sodium hydroxide – 1.2%, amount of sodium sulfate – 12%



Reaction conditions: amount of epoxy propane – 10%, reaction temperature – 40 °C, amount of sodium hydroxide – 1.2%, reaction time – 18 h

Figure 1: Effect of amount of epoxy propane (a), reaction temperature (b), reaction time (c), amount of sodium hydroxide (d) and sodium sulfate (e) on MS of HOHACS

Sodium hydroxide acted as a catalyst during the hydroxypropylation. From Figure 1d, it may be remarked that the amount of sodium hydroxide was varied from 0.8% to 1.6% to examine the effects of varying the amount of sodium hydroxide. The MS of HOHACS increased with increasing the amount of sodium hydroxide. The MS of HOHACS increased rapidly when the amount of sodium hydroxide was less than 1.2%, then slowed down when the amount of sodium hydroxide exceeded 1.2%. Thus, the most suitable amount of sodium hydroxide was considered to be 1.2%.

Sodium sulfate acted as inhibiting agent, preventing the swelling of starch particles during the hydroxypropylation, so that it was helpful for the post-processing of derivatives. From Figure 1e, the amount of sodium sulfate was varied from 6% to 14% to examine the effects of the amount of sodium sulfate. The MS of HOHACS increased with increasing the amount of sodium sulfate up to 10%. However, when the amount of sodium sulfate exceeded 10%, the MS of HOHACS decreased. It suggested that the high concentration of sodium sulfate in the slurry prevented the hydroxypropylation reaction of epoxy propane with OHACS. Therefore, the most suitable amount of sodium sulfate was considered to be 10%.

Optimization of technological parameters

Experimental design and results of response surface methodology

Based on the results of the single factor tests, the process parameters for preparing HOHACS were optimized using the MS as the response value by the Design-Expert software 8.05b. The actual values of the factors were selected at three levels. The design and results of the response surface testing are shown in Table 1.

Mathematical model and ANOVA analysis

Based on the Box–Behnken Design and the

results of the experiments, the second-order response surface model for preparing OHACS was as follows:

$$\begin{aligned} MS = & -0.89051 - 1.552 \times 10^{-3}A + 0.03504B - 1.1150 \times 10^{-4}C + 9.219 \times 10^{-3}D + 0.01077E + 6.842 \times 10^{-4}AB \\ & + 0.01393AC + 4.453 \times 10^{-4}AD + 5.719 \times 10^{-4}AE + 1.345 \times 10^{-3}BC + 8.000 \times 10^{-5}BD - 7.750 \times 10^{-5}BE \\ & - 1.606 \times 10^{-3}CD + 0.01480CE - 3.197 \times 10^{-4}DE - 2.490 \times 10^{-3}A^2 - 5.164 \times 10^{-4}B^2 - 0.09328C^2 - 2.602 \\ & \times 10^{-4}D^2 - 1.409 \times 10^{-3}E^2 \end{aligned} \quad (11)$$

The analysis of variance (ANOVA) was performed to check the significance of the fit of the second-order polynomial equation for the experimental data, and the results are given in Table 2.

Generally, the P-value was also used to check the significance of each coefficient. The smaller the P-value was, the more significant the corresponding coefficient was. From Table 2, the P value of the model was less than 0.0001 and the model was the most significant. It could be seen from Table 2 that the items of A, B, C, D, A², B² were statistically the most significant because their P-values were very small (P < 0.0001). The items of C², D², E², AB and AC were significant. According to ANOVA, the simplified equation can be described as follows:

$$\begin{aligned} MS = & -0.89051 - 1.552 \times 10^{-3}A + 0.03504B - 1.1150 \times 10^{-4}C + 9.219 \times 10^{-3}D + 6.842 \times 10^{-4}AB \\ & + 0.01393AC + 0.01480CE - 2.490 \times 10^{-3}A^2 - 5.164 \times 10^{-4}B^2 - 0.09328C^2 - 2.602 \\ & \times 10^{-4}D^2 - 1.409 \times 10^{-3}E^2 \end{aligned} \quad (12)$$

The goodness of the model fit was checked by the determination coefficient (R²). In this case, the determination coefficient (R²) was 0.9628. This implied that 96.28% of the variation could be explained by the regression model. Therefore, the model had high credibility. In addition, the value of the adjusted determination coefficient (R²_{Adj} = 0.9330) was also high and supported the high applicability of the model, which indicated the high precision and reliability of the experiments.²⁹

According to the F values in Table 2, the increasing order of the factors influencing the MS was as follows: the amount of epoxy propane, reaction temperature, the amount of sodium hydroxide, reaction time and the amount of sodium sulfate. Within the experimental range

studied, the optimal conditions for preparing HOHACS were predicted using the optimization

function of the Design Expert software.

Table 1
Box-Behnken test designs and corresponding results

Batch number	Amount of epoxy propane (A), %	Reaction temperature (B), °C	Amount of sodium hydroxide (C),%	Reaction time (D), h	Amount of sodium sulfate (E),%	MS
1	12	40	1.4	18	12	0.113
2	10	40	1.2	14	10	0.0777
3	10	40	1.4	18	10	0.103
4	10	40	1.4	22	8	0.0999
5	8	40	1.6	18	10	0.0760
6	10	40	1.2	22	10	0.0928
7	8	35	1.4	18	10	0.0501
8	10	40	1.4	22	12	0.0960
9	10	40	1.4	18	10	0.103
10	10	35	1.6	18	10	0.0844
11	10	40	1.4	18	10	0.103
12	10	40	1.2	18	8	0.0872
13	10	40	1.4	18	10	0.103
14	10	40	1.6	18	12	0.112
15	10	45	1.4	18	12	0.0981
16	8	40	1.4	18	8	0.0690
17	10	35	1.4	14	10	0.0645
18	10	40	1.4	18	10	0.103
19	8	40	1.4	14	10	0.0628
20	12	40	1.4	22	10	0.122
21	8	45	1.4	18	10	0.0750
22	10	35	1.4	18	8	0.0647
23	10	40	1.6	14	10	0.0953
24	10	40	1.6	22	10	0.105
25	10	35	1.2	18	10	0.0659
26	10	45	1.4	18	8	0.0974
27	10	45	1.4	14	10	0.0879
28	12	40	1.4	14	10	0.0903
29	12	45	1.4	18	10	0.122
30	12	40	1.6	18	10	0.123
31	10	45	1.4	22	10	0.113
32	10	40	1.4	14	8	0.0886
33	10	40	1.6	18	8	0.101
34	10	35	1.4	18	12	0.0680
35	8	40	1.2	18	10	0.0673
36	10	45	1.6	18	10	0.115
37	8	40	1.4	18	12	0.0642
38	12	40	1.4	18	8	0.109
39	10	40	1.2	18	12	0.0749
40	10	40	1.4	14	12	0.949
41	10	40	1.4	18	10	0.103
42	12	40	1.2	18	10	0.0917
43	10	35	1.4	22	10	0.0837
44	8	40	1.4	22	10	0.0805
45	10	45	1.2	18	10	0.0914
46	12	35	1.4	18	10	0.0697

The predicted optimum reaction conditions were:
amount of epoxy propane of 9.95%, reaction

temperature of 41.96 °C, amount of sodium hydroxide of 1.31%, reaction time of 17.58 h,

amount of sodium sulfate of 8.67%. Considering the feasibility of the practical operation, the optimum reaction conditions were adjusted as follows: amount of epoxy propane of 10%,

reaction temperature of 42 °C, amount of sodium hydroxide of 1.3%, reaction time of 17.5 h, amount of sodium sulfate of 9%.

Table 2
Analysis of variance for Box-Behnken parameter components

Source	Sum of squares	Degree of freedom	Mean square	F value	P value	Prob>F
Model	0.015	20	7.295×10 ⁻⁴	32.31	< 0.0001	**
A	5.492×10 ⁻³	1	5.492×10 ⁻³	243.26	< 0.0001	**
B	3.904×10 ⁻³	1	3.904×10 ⁻³	172.92	< 0.0001	**
C	1.659×10 ⁻³	1	1.659×10 ⁻³	73.49	< 0.0001	**
D	1.085×10 ⁻³	1	1.085×10 ⁻³	48.04	< 0.0001	**
E	1.918×10 ⁻⁶	1	1.918×10 ⁻⁶	0.085	0.7731	
A ²	8.655×10 ⁻⁴	1	8.655×10 ⁻⁴	38.33	< 0.0001	**
B ²	1.454×10 ⁻³	1	1.454×10 ⁻³	64.42	< 0.0001	**
C ²	1.215×10 ⁻⁴	1	1.215×10 ⁻⁴	5.38	0.0288	*
D ²	1.513×10 ⁻⁴	1	1.513×10 ⁻⁴	6.70	0.0158	*
E ²	2.773×10 ⁻⁴	1	2.773×10 ⁻⁴	12.28	0.0017	*
AB	1.873×10 ⁻⁴	1	1.873×10 ⁻⁴	8.29	0.008	*
AC	1.242×10 ⁻⁴	1	1.242×10 ⁻⁴	5.50	0.0272	*
AD	5.077×10 ⁻⁵	1	5.077×10 ⁻⁵	2.25	0.1463	
AE	2.093×10 ⁻⁵	1	2.093×10 ⁻⁵	0.93	0.3449	
BC	7.236×10 ⁻⁶	1	7.236×10 ⁻⁶	0.32	0.5764	
BD	1.024×10 ⁻⁵	1	1.024×10 ⁻⁵	0.45	0.5068	
BE	2.402×10 ⁻⁶	1	2.402×10 ⁻⁶	0.11	0.747	
CD	6.605×10 ⁻⁶	1	6.605×10 ⁻⁶	0.29	0.5934	
CE	1.402×10 ⁻⁴	1	1.402×10 ⁻⁴	6.21	0.0197	*
DE	2.616×10 ⁻⁵	1	2.616×10 ⁻⁵	1.16	0.292	
Residuals	5.644×10 ⁻⁴	25	2.258×10 ⁻⁵			
Lack of fit	5.644×10 ⁻⁴	20	2.822×10 ⁻⁵			
Pure error	0.000	5	0.000			
Cor. total	0.015	45				

* significant difference ($P < 0.05$); ** the most significant difference ($P < 0.001$)

Model verification

Under the adjusted optimum reaction conditions, the experiments were carried out three times. The result showed that the experimental value (MS = 0.101) was in agreement with the

predicted values (MS = 0.1) of the model within a 99% confidence interval. It suggested that the model was suitable for estimating the experimental values.

Effect of oxidation and hydroxypropylation on swelling power, blue value and freeze-thaw stability

The freeze-thaw stability, blue value and swelling power of corn starch (CS), HACS, OHACS, hydroxypropyl high-amylose corn starch (HHACS) and HOHACS are shown in Table 3. The swelling power reflects the interaction between starch and water. The freeze-thaw stability indicates the water-retention ability of starch molecules. The content of the amylose starch depends on the blue value. From Table 3, the oxidation increased the swelling power and blue value of HACS, but reduced its separated water percentage.

The hydroxypropylation increased the swelling power of HACS, but reduced its separated water percentage. The blue value was not basically influenced by the hydroxypropylation, obviously, its effect was similar to that of acetylation.³⁰ It confirmed that the oxidation of sodium hypochlorite could sever HACS molecular chains, but the hydroxypropylation could not cut off the molecular chains. The reduction in the separated water percentage indicated that the freeze-thaw stability of HACS could be improved by the oxidation and hydroxypropylation, and the

swelling power and freeze-thaw stability of HACS were lower than those of CS.

Effect of oxidation and hydroxypropylation on acid and alkali resistance

The acid and alkali resistance of CS, HACS, OHACS, HHACS and HOHACS is tabulated in Tables 4 and 5. As may be noted from Tables 4 and 5, after HACS was oxidized by sodium hypochlorite or hydroxypropylated by propylene oxide, the viscosity of the derivatives decreased, whereas the acid and alkaline resistance of the derivatives increased. It proved that the oxidation and hydroxypropylation could improve the acid and alkali resistance of HACS. The viscosity of CS, HACS, OHACS, HHACS and HOHACS decreased in acidic medium, but their viscosity increased in an alkali environment. Obviously, the viscosity of HACS was lower than that of CS according to Table 4. The acid resistance of starch and its derivatives increased in the order of HHACS > HOHACS > HACS > OHACS > CS. The alkali resistance of starch and its derivatives increased in the order of HOHACS > HHACS > OHACS > HACS > CS.

It suggests that the effect of oxidation and hydroxypropylation on acid resistance and on alkali resistance was not the same for HACS.

Table 3

Effect of oxidation and hydroxypropylation on freeze-thaw stability, blue value and swelling power of HACS

Samples	Separated water percentage, %	Blue value	Swelling power, %
CS	46.2±0.7 ^d	0.282±0.03 ^a	15.7±0.2 ^b
HACS	52.7±0.8 ^e	0.537±0.04 ^c	6.4±0.1 ^a
OHACS (CC = 1.1%)	35.6±0.6 ^b	0.725±0.05 ^b	20.6±0.3 ^{cd}
HHACS (MS = 0.1)	40.9±0.7 ^c	0.532±0.04 ^c	18.5±0.3 ^c
HOHACS (CC = 1.1%, MS = 0.1)	28.4±0.5 ^a	0.723±0.05 ^b	35.0±0.4 ^d

Data are means of triplicate analyses with standard deviation; means in the same column with different superscripts were significantly different at the 5% level

Table 4
Effect of oxidation and hydroxypropylation on acid resistance of HACS

Samples	Viscosity (pH 6.8), mPa·s	Viscosity (pH 3.0), mPa·s	Percentage of viscosity change, %
CS	70.5±1.4 ^{d,C}	50.6±1.0 ^{d,B}	28.2±2.0 ^c
HACS	30.8±0.6 ^{c,B}	23.2±0.5 ^{c,A}	24.7±2.2 ^b
OHACS (CC = 1.1%)	27.6±0.6 ^{bc,B}	19.9±0.4 ^{b,A}	27.9±2.2 ^c
HHACS (MS = 0.1)	25.4±0.5 ^{b,B}	20.3±0.4 ^{b,A}	20.1±2.0 ^a
HOHACS (CC = 1.1%, MS = 0.1)	20.6±0.4 ^{a,B}	16.1±0.3 ^{a,A}	21.9±2.0 ^a

Data are means of triplicate analyses with standard deviation; means in the same column with different superscript lowercase letters were significantly different at the 5% level; means in the same line with different superscript capital letters, except for percentage of viscosity change, were significantly different at the 5% level

Table 5
Effect of oxidation and hydroxypropylation on alkali resistance of HACS

Samples	Viscosity (pH 6.8), mPa·s	Viscosity (pH 10.0), mPa·s	Percentage of viscosity change, %
CS	70.5±1.4 ^{c,A}	93.6±1.9 ^{e,B}	32.8±2.1 ^d
HACS	30.8±0.6 ^{d,A}	38.2±0.8 ^{d,B}	24.0±2.2 ^c
OHACS (CC = 1.1%)	27.6±0.6 ^{cd,A}	33.1±0.7 ^{c,B}	19.9±2.1 ^b
HHACS (MS = 0.1)	25.4±0.5 ^{c,A}	30.2±0.6 ^{b,B}	18.9±2.0 ^b
HOHACS (CC = 1.1%, MS = 0.1)	20.6±0.4 ^{a,A}	22.3±0.4 ^{a,B}	8.2±2.0 ^a

Data are means of triplicate analyses with standard deviation; means in the same column with different superscript lowercase letters were significantly different at the 5% level; means in the same line with different superscript capital letters, except for percentage of viscosity change, were significantly different at the 5% level

Table 6
Effect of oxidation and hydroxypropylation on cold and hot viscosity stability of HACS

Samples	Cold viscosity stability, %	Hot viscosity stability, %
CS	50.6±2.2 ^{a,A}	70.2±2.1 ^{a,B}
HACS	60.9±2.1 ^{b,A}	80.4±2.1 ^{b,B}
OHACS (CC = 1.1%)	70.4±2.1 ^{c,A}	85.3±2.0 ^{d,B}
HHACS (MS = 0.1)	68.3±2.1 ^{c,A}	82.7±2.0 ^{c,B}
HOHACS (CC = 1.1%, MS = 0.1)	85.9±2.0 ^{d,A}	90.5±1.8 ^{e,B}

Data are means of triplicate analyses with standard deviation; means in the same column with different superscript lowercase letters were significantly different at the 5% level; means in the same line with different superscript capital letters were significantly different at the 5% level

The above fact proved that the oxidation and hydroxypropylation could improve the acid and alkali resistance of HACS.

Effect of oxidation and hydroxypropylation on cold and hot viscosity stability

The cold and hot viscosity stability values of CS, HACS, OHACS, HHACS and HOHACS are listed in Table 6. From Table 6, it may be concluded that the cold viscosity stability and hot viscosity stability values of HACS are higher than those of CS. The cold viscosity stability and hot viscosity stability of OHACS, HHACS and HOHACS are higher than those of HACS.

It proved that the oxidation and hydroxypropylation could improve the cold and hot viscosity stability of HACS. For HACS and its derivatives, the contribution of the oxidation and hydroxypropylation to the hot viscosity stability was greater than to the cold viscosity stability.

FTIR analysis

The FTIR spectra of HACS, OHACS (CC = 1.103%) and HOHACS (MS = 0.1, CC = 1.103%) are shown in Figure 2. As may be remarked, the FTIR spectra of HACS, OHACS and HOHACS had similar profiles with some subtle differences. The absorption peak at the wavenumber of 3400 cm^{-1} belongs to the stretching vibration of $-\text{OH}$ groups, and the peak at the wavenumber of 2930 cm^{-1} belongs to the stretching vibration of C-H bonds.³¹ The absorption peaks at 1076 cm^{-1} and 1026 cm^{-1} correspond to the $-\text{C}-\text{O}-\text{C}$ stretching vibration.³² The CH_2 scissoring and CH_2 twisting bands appear at 1450 cm^{-1} and 1324 cm^{-1} , respectively. In the wavenumber range from 4000 cm^{-1} to 1590 cm^{-1} , the FTIR spectra curves of HOHACS are somewhere between those of HACS and OHACS.

The absorption peak of OHACS and HOHACS at the wavenumber of 1730 cm^{-1} is the characteristic peak of the carbonyl groups.^{33,34} It proves that the carboxyl groups were introduced into starch molecules, owing to the oxidation. The introduction of the hydroxypropyl groups could not obviously change the FTIR spectra of HACS.

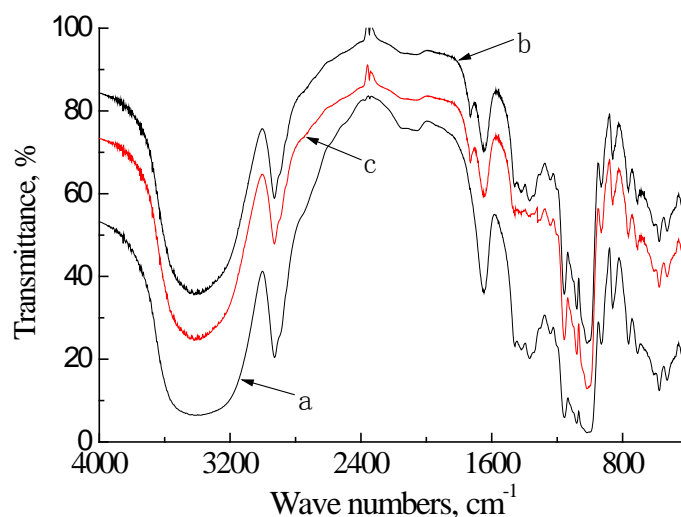


Figure 2: FTIR spectra of HACS (a), OHACS (b) and HOHACS (c)

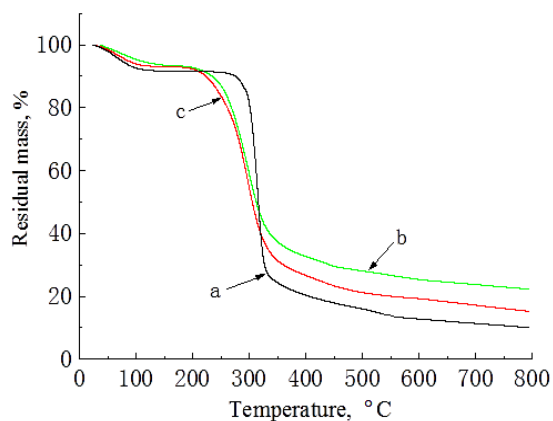


Figure 3: TGA curves of HACS (a), OHACS (b) and HOHACS (c)

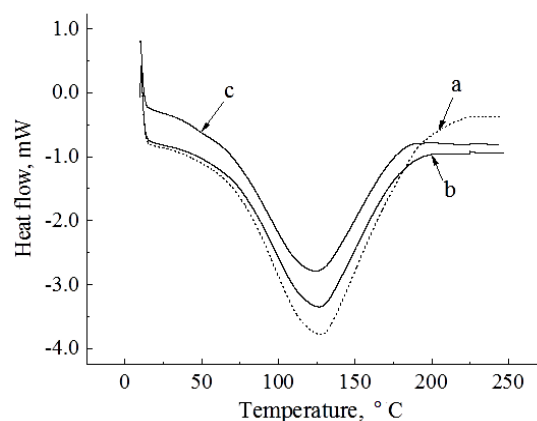


Figure 4: DSC curves of HACS (a), OHACS (b) and HOHACS (c)

TGA and DSC analyses

The TGA and DSC curves of HACS, OHACS (CC = 1.103%) and HOHACS (MS = 0.1, CC = 1.103%) are shown in Figures 3 and 4, respectively. The TGA and DSC curves of HOHACS and OHACS are obviously different from those of HACS, owing to oxidation and hydroxypropylation (Figs. 3 and 4), which altered the thermal stability and melting process of HACS. The TGA curves of HOHACS and OHACS intersected that of HACS at temperatures of 320.4 °C and 316.1 °C, respectively. When the temperature exceeded 320.4 °C, a part of the TGA curve of HOHACS was located somewhere between those of OHACS and HACS, which meant that the thermal stability of HOHACS was somewhere between those of OHACS and HACS.

Meanwhile, the thermal stability of OHACS was the highest of the three materials when the temperature exceeded 320.4 °C. It proved that the thermal stability of HACS was closely related to the introduction of the carboxyl groups and hydroxypropyl groups into the starch molecules. Finally, to compare these changes, the corresponding onset decomposition, end decomposition temperature, rate of mass loss, onset temperature, peak temperature, end temperature and melting enthalpy of HACS,

OHACS and HOHACS were listed in Table 7 and Table 8.

From Table 7, it can be remarked that the onset decomposition temperature for starch and its derivatives increased in the following order: OHACS, HOHACS, HACS. The end decomposition temperature of starch and its derivatives increased in the order of HACS, HOHACS, OHACS.

The oxidation could obviously reduce the onset decomposition temperature of HACS, but dramatically increased the end decomposition temperature of HACS according to the data in Table 7. Similarly, the hydroxypropylation could increase the onset decomposition temperature of OHACS, but decreased the end decomposition temperature of OHACS. The decrease in the onset decomposition temperature caused by the oxidation could be explained by the depolymerization of the molecular chains. The rate of the mass loss of HACS was greater than that of OHACS and HOHACS.

The rate of the mass loss of HOHACS was close to that of OHACS. This suggested that the oxidation improved the thermal stability of HACS, while the hydroxypropylation had a little contribution to it.

From Table 8, the introduction of the carboxyl groups resulted in the reduction in the onset temperature, peak temperature, end temperature and melting enthalpy of HACS. The reason was still ascribed to the depolymerization of the molecular chains. The introduction of

hydroxypropyl groups further reduced the onset temperature, peak temperature, end temperature and melting enthalpy of HACS, suggesting that the hydroxypropyl groups might weaken the hydrogen bonds between the molecular chains.

Table 7

Onset decomposition temperature, end decomposition temperature and mass loss rate of the samples

Samples	Onset decomposition temperature, °C	End decomposition temperature, °C	Rate of mass loss, %
HACS	300.4±3.0 ^c	326.7±3.3 ^a	50.8±0.6 ^b
OHACS	250.2±2.8 ^a	340.6±3.4 ^b	48.0±0.6 ^a
HOHACS	255.0±2.8 ^b	339.2±3.4 ^b	48.7±0.6 ^a

Data are means of triplicate analyses with standard deviation; means in the same column with different superscript lowercase letters were significantly different at the 5% level

Table 8

Onset temperature, peak temperature, end temperature and enthalpy change of the samples

Samples	Onset temperature, °C	Peak temperature, °C	End temperature, °C	Enthalpy change, J·g ⁻¹
HACS	73.0±0.9 ^c	127.8±1.3 ^a	194.2±2.2 ^c	265.5±3.6 ^c
OHACS	67.5±0.9 ^b	126.4±1.3 ^a	180.5±2.0 ^b	244.6±2.9 ^b
HOHACS	65.0±0.9 ^a	125.9±1.3 ^a	177.3±2.0 ^a	220.4±2.6 ^a

Data are means of triplicate analyses with standard deviation; means in the same column with different superscripts were significantly different at the 5% level

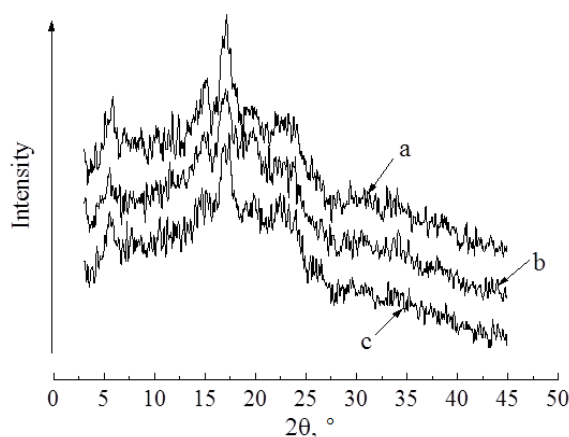


Figure 5: XRD patterns of HACS (a), OHACS (b) and HOHACS (c)

Effect of oxidation and hydroxypropylation on crystallinity degrees

The XRD patterns obtained for HACS, OHACS (CC = 1.103%) and HOHACS (MS = 0.1, CC = 1.103%) are shown in Figure 5. The diffractograms of HACS, OHACS and HOHACS reveal peaks at 5.6°, 15.2°, 17.3°, 19.9°, 22.1° and 23.8°, respectively, which should belong to the B type.³⁵ For OHACS and HOHACS, the intensity of the doublet observed around 15.2° and 17.3° was reduced by the oxidation. It suggested that the oxidation influenced the structure of HACS particles.

According to the XRD patterns, the area was calculated by MDI Jade 6.0 software. The crystallinity degrees (CD) of the HACS, OHACS and HOHACS were 28.2%, 25.4% and 24.9%, respectively. According to these data, the crystallinity degree of OHACS was more influenced by oxidation than by

hydroxypropylation. It confirmed that the oxidation mainly occurred in the crystalline region, while the hydroxypropylation mainly occurred in the amorphous region.

Particle morphology and energy dispersive X-ray analysis (EDAX)

The particle morphology and energy dispersive X-ray analysis of HACS, OHACS (CC = 1.103%) and HOHACS (MS = 0.1, CC = 1.103%) are illustrated in Figures 6 and 7, respectively. From Figure 6, no noticeable differences in the morphology of HACS and OHACS are observed. This suggests that the oxidation used in the present study did not cause any significant changes in the size and morphology of HACS particles. After OHACS was hydroxypropylated, however, the surface of the particles became rough.

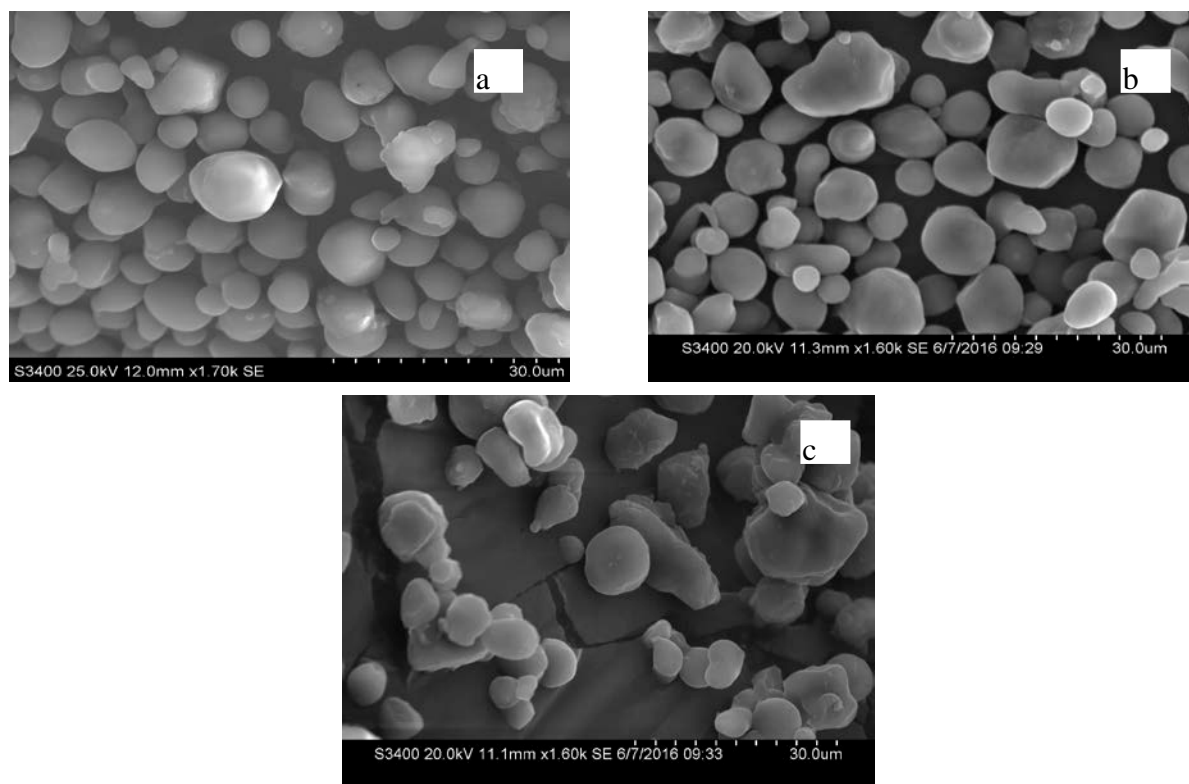


Figure 6: SEM of HACS (a), OHACS (b) and HOHACS (c)

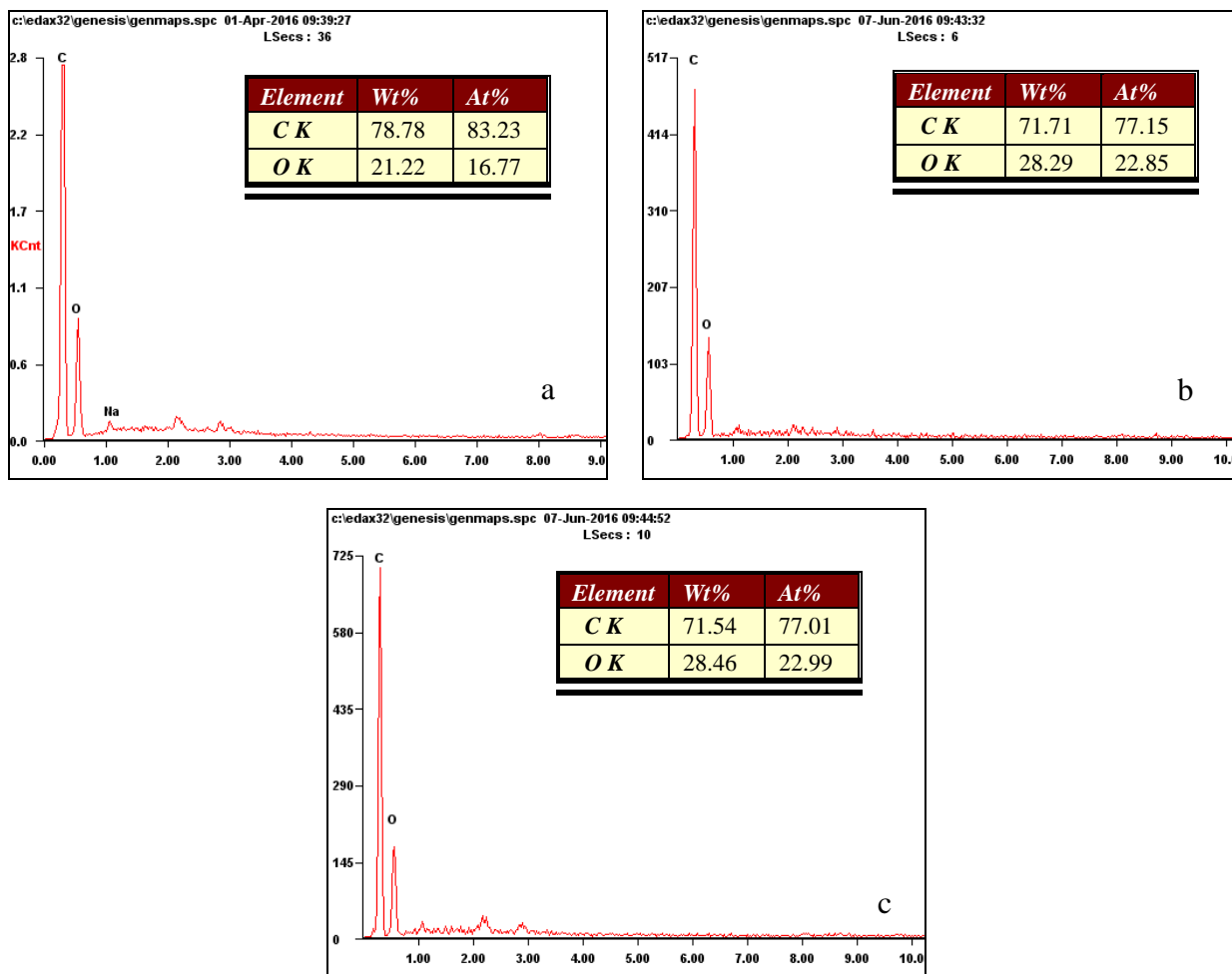


Figure 7: EDS of HACS (a), OHACS (b) and HOHACS (c)

The rough regions are mostly located on the side faces of the granules. It proves that the mechanism of the oxidation was different from that of the hydroxypropylation for HACS. The amorphous region of HACS granules is mainly located on the side faces, in agreement with the XRD results. Moreover, the hydroxypropylation occurred unevenly on the granules.

From Figure 7, it may be noted that after HACS was oxidized, the oxygen atom content increased obviously. It further proved that the carboxyl groups were introduced into the molecules of HACS. After OHACS was hydroxypropylated, the change in the content of carbon atoms and oxygen atoms was not so obvious.

CONCLUSION

The optimum conditions for preparing HOHACS were the following: amount of epoxy propane of 10%, reaction temperature of 42 °C, amount of sodium hydroxide of 1.3%, reaction time of 17.5 h and amount of sodium sulfate of 9%. The most significant factor was found to be the amount of epoxy propane, followed by the reaction temperature, the amount of sodium hydroxide, the reaction time and finally the amount of sodium sulfate.

The crystalline structure of HACS belonged to the B type. Oxidation occurred within the crystalline region, while hydroxypropylation occurred unevenly on the granules. The oxidation with sodium hypochlorite severed the molecular

chains of HACS, while the hydroxypropylation did not. Thus, the crystallinity degree of HOHACS was little affected by the hydroxypropylation.

Both treatments improved the freeze-thaw stability, acid and alkali resistance, cold and hot viscosity stability of HACS, as well as increased its swelling power. The hot viscosity stability of HACS was greatly influenced by the oxidation and hydroxypropylation, compared with the cold viscosity stability. The oxidation obviously reduced the onset decomposition temperature of HACS, but dramatically increased its end decomposition temperature.

The hydroxypropylation increased the onset decomposition temperature of OHACS, but decreased its end decomposition temperature. The introduction of the carboxyl and hydroxypropyl groups resulted in a reduction of the onset temperature, peak temperature, end temperature and melting enthalpy of HACS. Considering the improvement in the performance of the materials developed in this work, the findings of the present study can provide new insights into the research on the use of starch derivatives in food packages, ion chelation and drug delivery systems.

ACKNOWLEDGMENTS: We are grateful to our colleagues for their help in completing some of the experiments.

REFERENCES

- ¹ A. Serrero, S. Trombotto, P. Cassagnau, Y. Bayon, P. Gravagna *et al.*, *Biomacromolecules*, **11**, 1534 (2010).
- ² F. F. Takizawa, G. D. O. D. Silva, F. E. Konkel and I. M. Demiate, *Braz. Arch. Biol. Technol.*, **47**, 921 (2004).
- ³ P. Myllärinen, R. Partanen, J. Seppälä and P. Forssell, *Carbohydr. Polym.*, **50**, 355 (2002).
- ⁴ Y. J. Wang and L. Wang, *Carbohydr. Polym.*, **52**, 207 (2003).

- ⁵ D. Kuakpetoon and Y. J. Wang, *Carbohydr. Res.*, **343**, 90 (2008).
- ⁶ M. A. El-Sheikh, M. A. Ramadan and A. El-Shafie, *Carbohydr. Polym.*, **80**, 266 (2010).
- ⁷ O. S. Lawal, *Food Chem.*, **87**, 205 (2004).
- ⁸ K. S. Sandhu, M. Kaur, N. Singh and S. T. Lim, *LWT-Food Sci. Technol.*, **41**, 1000 (2008).
- ⁹ A. Gunaratne and H. Corke, *Carbohydr. Polym.*, **68**, 305 (2007).
- ¹⁰ D. Kuakpetoon and Y. J. Wang, *Carbohydr. Res.*, **341**, 1896 (2006).
- ¹¹ H. L. Lee and B. Yoo, *LWT-Food Sci. Technol.*, **44**, 765 (2011).
- ¹² O. S. Lawal, K. O. Adebawale, B. M. Ogunsanwo, L. L. Barba and N. S. Ilo, *Int. J. Biol. Macromol.*, **35**, 71 (2005).
- ¹³ P. Naknaen, *Food Biophys.*, **9**, 249 (2014).
- ¹⁴ K. N. Awokoya, L. M. Nwokocha, B. A. Moronkola and D. O. Moronkola, *Der Chem. Sinica*, **2**, 228 (2011).
- ¹⁵ S. F. Yu, Y. Ma, L. Menager and D. W. Sun, *Food Bioprocess Technol.*, **5**, 626 (2012).
- ¹⁶ C. S. Raina, S. Singh, A. S. Bawa and D. C. Saxena, *Eur. Food Res. Technol.*, **223**, 561 (2006).
- ¹⁷ J. Tattiyaku, P. Pradipasena and S. Asavasaksakul, *Starch/Stärke*, **59**, 342 (2007).
- ¹⁸ Đ. Ačkar, D. Šubarić, J. Babić, B. Miličević and A. Jozinović, *J. Food Sci. Technol.*, **51**, 1463 (2014).
- ¹⁹ S. Balasubramanian, R. Sharma, J. Kaur and N. Bhardwaj, *J. Food Sci. Technol.* **51**, 294 (2014).
- ²⁰ R. C. Yuan and D. B. Thompson, *Cereal Chem.*, **75**, 571 (1998).
- ²¹ Q. Wang, P. R. Ellis and S. B. Ross-Murphy, *Food Hydrocoll.*, **14**, 129 (2000).
- ²² H. B. Tang, Y. P. Li, M. Sun and X. G. Wang, *Polym. J.*, **44**, 211 (2012).
- ²³ M. Černá, A. S. Barros, A. Nunes, S. M. Rocha, I. Delgadillo *et al.*, *Carbohydr. Polym.*, **51**, 383 (2003).
- ²⁴ C. O. Akintayo and E. T. Akintayo, *Adv. Nat. Appl. Sci.*, **3**, 196 (2009).
- ²⁵ M. M. Sánchez-Rivera, I. Flores-Ramírez, P. B. Zamudio-Flores, R. A. González-Soto, S. L.

- Rodríguez-Ambríz *et al.*, *Starch/Stärke*, **62**, 155 (2010).
- ²⁶ K. S. Sandhu and N. Singh, *Food Chem.*, **101**, 1499 (2007).
- ²⁷ S. Nara and T. Komiya, *Starch/Stärke*, **35**, 407 (1983).
- ²⁸ H. X. Xiao, Q. L. Lin, G. Q. Liu and F. X. Yu, *Molecules*, **17**, 10946 (2012).
- ²⁹ R. Lin, H. Li, H. Long, J. Su, W. Huang *et al.*, *J. Mol. Catal. B*, **105**, 104 (2014).
- ³⁰ M. Sun, H. Tang and Y. Li, *Cellulose Chem. Technol.*, **51**, 929 (2017).
- ³¹ D. Kalita, N. Kaushik and C. L. Mahanta, *J. Food Sci. Technol.*, **51**, 2790 (2014).
- ³² S. D. Zhang, Y. R. Zhang, H. X. Huang, B. Y. Yan, X. Zhang *et al.*, *J. Polym. Res.*, **17**, 43 (2010).
- ³³ D. K. Kweon, J. K. Choi, E. K. Kim and S. T. Lim, *Carbohydr. Polym.*, **46**, 171 (2001).
- ³⁴ A. Para, *Carbohydr. Polym.*, **57**, 277 (2004).
- ³⁵ X. Ma, R. Jian, P. R. Chang and J. Yu, *Biomacromolecules*, **9**, 3314 (2008).